
About Explicit Variance Minimization: Training Neural Networks for Medical Imaging With Limited Data Annotations.

Dmitrii Shubin ^{1,2}

Toronto, Canada

dmitrii.shubin@mail.utoronto.ca

Danny Eytan ^{2,3}

Haifa, Israel

danny.eytan@sickkids.ca

Sebastian D. Goodfellow ^{1,2}

Toronto, Canada

sebastian.goodfellow@utoronto.ca

¹Faculty of Applied Science and Engineering, University of Toronto

²Department of Critical Care Medicine, The Hospital for Sick Children

³Faculty of Medicine, Technion

Abstract

Self-supervised learning methods for computer vision have demonstrated the effectiveness of pre-training feature representations, resulting in well-generalizing Deep Neural Networks, even if the annotated data are limited. However, representation learning techniques require a significant amount of time for model training, with most of it time spent on precise hyper-parameter optimization and selection of augmentation techniques. We hypothesized that if the annotated dataset has enough morphological diversity to capture the general population's as is common in medical imaging, for example, due to conserved similarities of tissue mythologies, the variance error of the trained model is the prevalent component of the Bias-Variance Trade-off. We propose the Variance Aware Training (VAT) method that exploits this property by introducing the variance error into the model loss function, i.e., enabling minimizing the variance *explicitly*. Additionally, we provide the theoretical formulation and proof of the proposed method to aid in interpreting the approach. Our method requires selecting only one hyper-parameter and was able to match or improve the state-of-the-art performance of self-supervised methods while achieving an order of magnitude reduction in the GPU training time. We validated VAT on three medical imaging datasets from diverse domains and various learning objectives. These included a Magnetic Resonance Imaging (MRI) dataset for the heart semantic segmentation (MICCAI 2017 ACDC challenge), fundus photography dataset for ordinary regression of diabetic retinopathy progression (Kaggle 2019 APTOS Blindness Detection challenge), and classification of histopathologic scans of lymph node sections (PatchCamelyon dataset).

1 Introduction

Limited data annotation is a mainstream problem for medical imaging due to the high cost of the annotation procedure, which creates challenges in cross-subject generalization. Various domain adaptation methods have been proposed to address this issue, such as Semi-Supervised (SeSL) methods [31, 14, 37] and a broad set of Self-Supervised (SSL) methods based on learning semantic similarity [30, 10], context understanding [17, 41, 13, 39, 23, 19, 9], and medical imaging domain properties [16, 22, 35, 42, 29].

While SeSL methods are time-consuming in general, requiring backpropagation through the entire dataset over multiple iterations, SSL methods are sensitive to the selection of correct augmentation transformations, making it time-consuming concerning hyper-parameter optimization.

Our motivation stems from the field of machine learning in healthcare, and specifically medical imaging. While not unique to the medical field, there are two typical attributes of associated datasets that suggest alternative approaches to pre-training might be beneficial: the limited amount of well-labelled data, and often relatively low inter-subject and inter-subset variability compared to the entire population distribution. For example, the image acquisition protocols are conserved across institutions, there are limited vendors and types of devices, and for a given imaging interpretation task, there are a limited number of underlying pathological processes. This skewed partition of the overall variance suggests that a relatively small sample of the population might capture most of the total variance, and a learning algorithm that can be tuned according to this property might still be as effective while requiring much less compute resources than a more brute force approach.

Following this assumption, we hypothesize that the limited dataset size causes the variance error to be the dominant component in Bias-Variance Trade-off Decomposition (BVTd). A common approach to reducing the variance of a Deep Neural Network (DNN) is to introduce regularisation into the model, such as dropout [7] or weighted decay. The major disadvantage of such methods is they reduce the explicit power of the model. In contrast, we propose a method that explicitly optimizes the variance, where the variance of the model is minimized directly as a part of the model's cost function, which introduces the constrain into the model without the loss of capacity.

Our work presents three major contributions. In Section 3.1, we propose a theorem describing the model's variance error behaviour and propose the objective function that enables explicit variance error optimization. By adopting and combining ideas from Generative Adversarial [5], Domain Adversarial [45], and Siamese Neural Networks [2], in Section 3.2 we propose the Variance-Aware Training (VAT) method, which is a time-efficient method for training generalized Convolution Neural Networks (CNN). Lastly, In Section 4, we provided benchmarks to quantify the performance of the proposed method and provided an interpretation based on the theoretical background.

2 Related work

Prior theoretical work provided by Neal et al. [20] and Yang et al. [38] analyzed techniques for measuring the Bias-Variance Trade-off components of Deep Neural Networks. In this paper, we provided an alternative perspective to the BVTd, which is to consider it as the decomposition of the universal approximate error. Additionally, we have translated the described theoretical background into the novel variance-aware arbitrary loss function, that can be used to minimize the variance directly.

Fundamentally, our work is based on the principles described by Goodfellow et al. [5] (2014) for Generative Adversarial Networks (GAN), where the mechanism of minimizing the nonconformity between the distribution of real images and images generated by the generative neural network G via backpropagation of the error from the discriminative network D .

In particular, our method is a special case of Domain-Adversarial Networks (DAN), which were introduced by Ganin et al. [45] (2016) and extended in applications by Kim et al. [25]. DAN is designed to minimize a gap between two datasets from various domains using a Reversed Gradient Layer (RGL) to reverse all gradients passed through it. In our method, we used RGL to minimize a gap between training and validation subsets thus, minimizing the variance of the model. Additionally, unlike the original DAN, we introduced our own computationally efficient feature map estimates to penalize both local and global feature representations.

As a feature extractor for our training method, we used the Siamese Neural Network (SNN) architecture proposed by Bromley et al. [2] (1994). SNN was designed for learning feature representations as a similarity between a pair of two samples through feature extractors with shared weights. Several later works proposed an extension of the method to the imaging data [4], and afterward, diverse loss functions [40, 32, 6] for applications such as face identification [12], processing sets of elements [34, 18] and object tracking [21, 26, 28].

3 Variance-Aware Training

3.1 About explicit minimization of the variance error

We summarized the generic theoretical background of the proposed DNN training method in the following theorem:

Theorem 1. \bar{P}, \hat{P}, Q are distributions of the feature representations in training, validation and testing subsets, respectively. Neural network G is a compact universal approximation of Q ($\|\cdot\|_\infty$) with a set of trainable parameters θ when the optimization objective of G is defined as follows:

$$\max_{\bar{P}_x} \left[\bar{P}_x(\hat{y} = y|x, \theta) - \lambda D_{KL}(\hat{P}_x \| \bar{P}_x) \right]$$

Proof. According to the The Universal Approximation Theorem [1, 33]:

$$\exists G : \sup_{x \in R^n} |\mathbb{E}[G(x)] - \mathbb{E}[f(x)]| < \epsilon, \epsilon \rightarrow 0 \quad \forall f : R^n \rightarrow R^m \quad \forall x \in R^n \quad (1)$$

where f is an arbitrary polynomial function. By definition, Equation 1 expresses the Total Distance of Probability Measures (TDPM) between $\mathbb{E}[G(x)]$ and $\mathbb{E}[f(x)]$. Following Pinsker's inequality, the TDPM is upper bounded by the Kullback–Leibler (KL) divergence of the estimated feature representations (Equation 2). Thereby, minimization of the KL divergence leads to minimization of the TDPM between the f and its approximation G (Equation 3,4).

$$\sup_{x \in R^n} |\mathbb{E}[f(x)] - \mathbb{E}[G(x)]| \leq \sqrt{\frac{1}{2} D_{KL}(\mathbb{E}[f(x)] \| \mathbb{E}[G(x)])} \quad (2)$$

$$\min_{x \in R^n} \|\mathbb{E}[f(x)] - \mathbb{E}[G(x)]\|_1 \iff \min_{x \in R^n} D_{KL}(\mathbb{E}[f(x)] \| \mathbb{E}[G(x)]) \quad (3)$$

$$\min_{x \in R^n} \|Q_x - \bar{P}_x\|_1 \iff \min_{x \in R^n} D_{KL}(Q_x \| \bar{P}_x) \quad (4)$$

The expectation of the error $\mathbb{E}[D_{KL}(Q_x \| \bar{P}_x)]$ is characterised by the BVTD [3] (Equation 5), where \bar{P}_x represents the likelihood approximated by G on the training subset, \hat{P}_x represents the likelihood estimated by G on the validation subset, which is also specified as an average distribution $\hat{P}_x = \frac{1}{2}(\bar{P}_x + Q_x)$, and Q_x represents the likelihood derived from the testing subset (general population).

$$\mathbb{E} [D_{KL}(Q_x \| \bar{P}_x)] = \underbrace{D_{KL}(Q_x \| \hat{P}_x)}_{\text{Bias error}} + \underbrace{\mathbb{E}[D_{KL}(\hat{P}_x \| \bar{P}_x)]}_{\text{Variance error}} + \sum_i^N \underbrace{Q_{x_i} \log(Q_{x_i})}_{\text{Bayes error}} \quad (5)$$

$$\max_{\bar{P}_x} \left[\bar{P}_x(\hat{y} = y|x, \theta) - \lambda D_{KL}(\hat{P}_x \| \bar{P}_x) \right] \quad (6)$$

In a real-world setting, Q_x can not be observed for direct parametric optimization by a DNN, assuming that the test subset represents the general population. Even if some portion of the testing subset \hat{Q}_x is representable, i.e., $\lim_{x \rightarrow \infty} \frac{\hat{Q}_x}{Q_x} = 1$, it can still only be used for the final evaluation of G to keep the integrity of the cross-validation procedure. Further, the bias error component of the BVTD can not be minimized explicitly. In contrast, the variance term can be optimized *explicitly* by introducing $D_{KL}(\hat{P}_x \| \bar{P}_x)$ as an additional constraint into the objective function. After applying Lagrangian relaxation, the resulting multi-task objective of the DNN is characterized by Equation 6.

The proof of Theorem 1 presents several intuitive observations. Firstly, we demonstrate that minimizing the KL divergence between training and validation subsets is equivalent to explicit minimisation of the model's variance error. Moreover, the explicit minimization only requires matching learned

likelihood distributions without prior knowledge of targets (i.e., CNN feature activation map distributions), which maintains cross-validation integrity. Therefore, explicit variance minimization implicitly leads to minimization of the gap between the DNN and the asymptotic approximation of the data’s inherent likelihood.

Secondly, since the two losses in the optimization objective are controversial, the auxiliary KL divergence loss function characterizes the explicit regularization of G , parameterized by mixing coefficient λ . Introducing variance into the cost function increases the degrees of freedom of the optimization objective, leading the model to find an optimal min-max equilibrium of the bias and variance error components in Equation 5. Accordingly, we explored the relationship between the parameter λ and the resulting model’s error and provided experimental results in Section 4.

Lastly, we demonstrated that the bias error component could be only minimized implicitly. If the morphological diversity of \bar{P}_x is not sufficient to express the diversity of the feature representations in Q_x , the bias component becomes the prevailing component in the BVTD, which is a limitation for proposed method.

3.2 Model Architecture

Note that instead of sampling images x_a from the validation subset, described in Theorem 1, Algorithm 1 implies sampling from the pre-training subset X_{Pre} . We assume that X_{Pre} includes more data samples and samples of more diverse spatial morphology, resulting in improved generalization.

$$L_{total} = L_{main}(t_{tr}, \hat{t}_{tr}) + \lambda BCE(t_a, \hat{t}_a) \quad (7)$$

Previous research on adversarial domain adaptation [45, 25] describes a model architecture where the adversarial network is connected to the last feature embedding layer that conveys the global feature representations $e_k(x)$. However, the theoretical proof of VAT implies penalizing *all* layers of the network. At the same time, penalizing only global feature representations results in an optimization

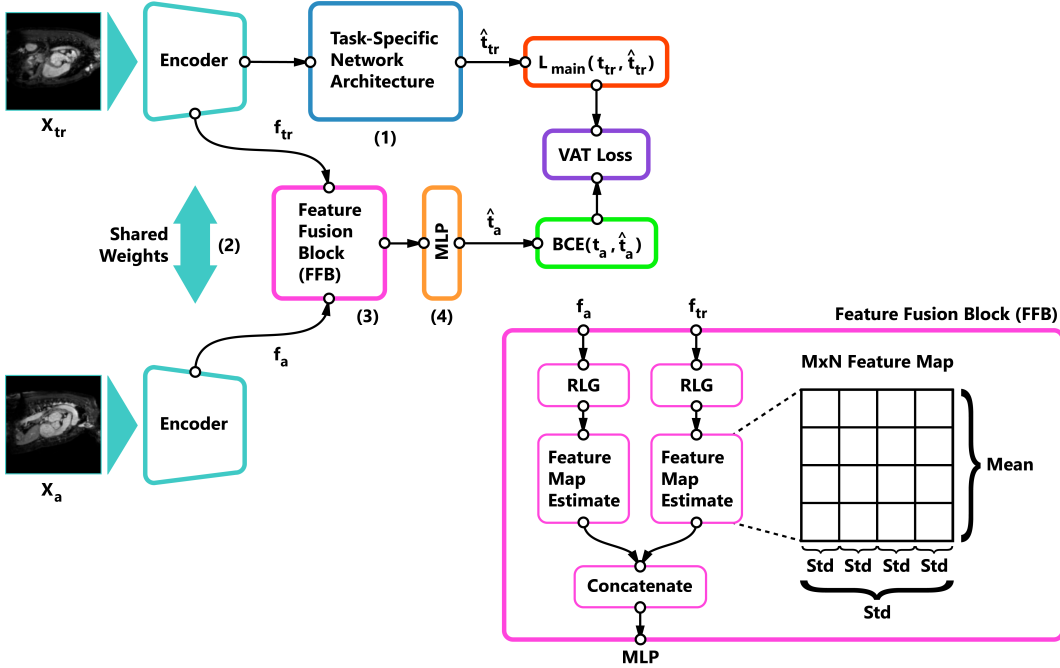
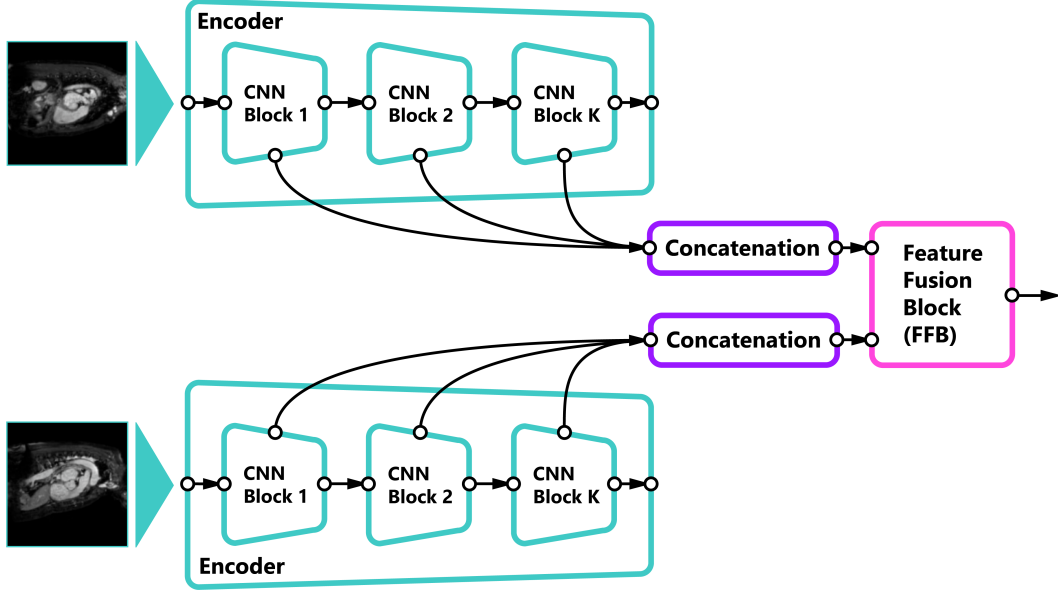


Figure 1: Generic structure of Variance-Aware Training framework. MLP (4) is tasked to classify if 2 images are part of the same subset (training or pre-training). Due to incorporated RGL layers, all gradients that lead to distinguishing subsets will be reversed, which leads to forgetting subset-specific information, i.e. explicit minimization of the model variance. After training, only main network (1) will be used for inference.

(a) Early Aggregation



(b) Late Aggregation

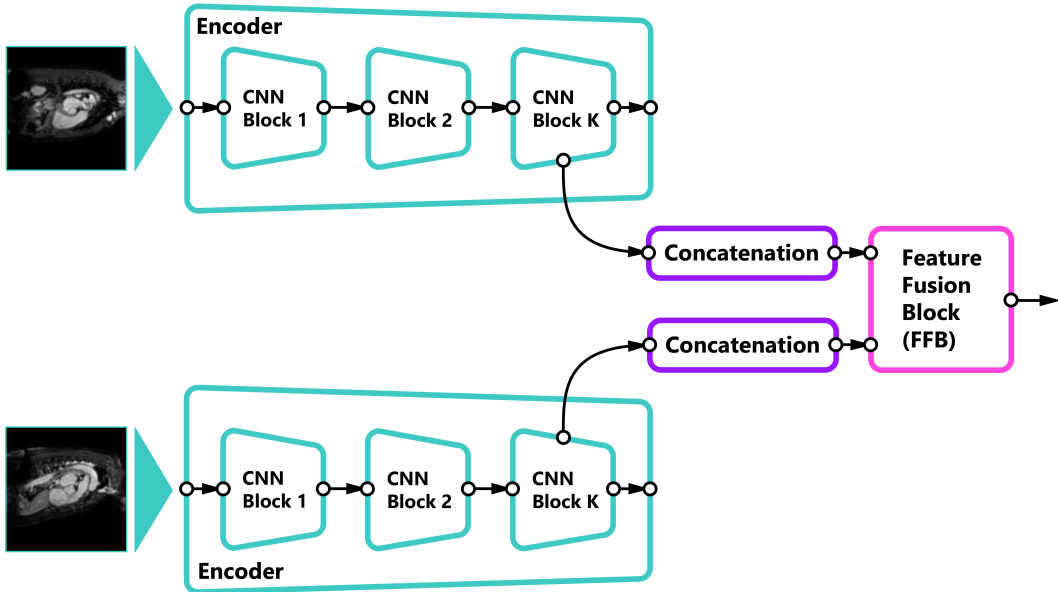


Figure 2: Proposed alternatives for aggregation methods: (a) early aggregation when all layers from the encoder are penalized by VAT, (b) late aggregation when only global feature representations are penalized.

issue for our method because the information flow tends to avoid introduced adversarial constraints on the loss surface. To explore this effect, we propose two types of fusion: early aggregation where feature maps (f_{tr}, f_a) from all CNN blocks are connected to the FFB, and late aggregation ($e_k(x_i), e_k(x_a)$), which is similar to previous studies [45, 25] (Figure 2). The early aggregation method with K CNN block requires K Local Reparameterization Tricks [8] to backpropagate through

a random node. This could be computationally expensive and therefore, we replaced it with parametric statistical estimates (Figure 1) to overcome this problem.

Similar to SSL methods, only the main network S will be used for final inference after VAT, which will not increase the computational and space requirements of the resulting base neural network.

Algorithm 1: Sampling of the auxiliary image x_a

Result: x_a, t_a

$x_{tr} \in X_{tr}$

X_{pre}

$a \leftarrow Uniform[0, 1]$

Instructions:

if $a \leq 0.5$ **then**

$x_a \in X_{tr}, x_a \neq x_{tr}$

$t_a = 1$

else

$x_a \in X_{pre}$

$t_a = 0$

4 Experiments

4.1 Experimental setup

Datasets: We evaluated the proposed method on 3 diverse tasks using publicly available medical imaging datasets. (1) The ACDC semantic segmentation dataset [44] includes 100 volumetric images of 1.5T and 3T MRI scans with three expert-annotated structures: left ventricle, myocardium, and right ventricle. (2) The APTOS 2019 dataset [43] includes 3662 fundus photography images for ordinary regression of the diabetic retinopathy progression: healthy condition, mild, moderate, severe, and proliferative. (3) PatchCamelyon (PCam) dataset [15] includes 220025 low-resolution histopathologic scans of lymph node sections for classification of healthy and metastatic tissues. We summarized the qualitative and quantitative specifications of datasets in Table 1.

Base model: We used a 6-layer 2D Dense U-Net [24] constrained by the smoothed Dice macro loss function as a base architecture for semantic segmentation experiments (ACDC). The EfficientNet-b3 [27] model, constrained by the mean absolute error and Binary Cross-Entropy loss functions, was used for ordinary regression (APTOS) and classification (PCam) experiments respectively. EfficientNet-b3

Table 1: Summarised description of experimental datasets.

Characteristic	ACDC	APTOS	PCam
Domain	MRI images	Fundus photography	Histopathologic scans
Learning objective	Semantic segmentation	Ordinary regression	Binary classification
Color map	Grayscale	RGB	RGB
Spatial correlation between samples	Yes (3D scans)	No	No
Population	Healthy, previous myocardial infarction, dilated cardiomyopathy, hypertrophic cardiomyopathy, abnormal right ventricle	Healthy, mild, moderate, severe, proliferative retinopathy	Metastatic and normal tissues
Morphological features	Small and large adjacent segments, variability of patterns between patients populations	Variety of abnormal tissues	Low resolution
Number of samples	100 volumes (1902 slices)	3662 images	220025 images

was pre-trained on the ImageNet dataset. All of our models were trained using the Adam optimizer [11] with a learning rate of 0.001 and batch size of 32. For SSL tasks, we optimized the model for 1000 epochs. For downstream SSL tasks, fully supervised and VAT, we optimized models for 3000 epochs.

Pre-processing: Similar to [36], we applied a circular crop to APTOS images and selected only the eye zone to prevent over-fitting on image borders. For the APTOS and PCam datasets, before feeding the image into the model, we applied normalization using ImageNet coefficients (mean: 0.485, 0.456, 0.406; standard deviation: 0.229, 0.224, 0.225). For the ACDC dataset, we applied channel-wise standard scaling to the images. Images from the ACDC and APTOS datasets were reshaped to resolutions of 154x154 and 256x256, respectively. The optimal set of rigid and non-rigid augmentations were manually determined for all experiments. For the ACDC dataset, we used horizontal flip, random rotation, elastic transform, random crop, and random gamma augmentations. For the APTOS and PCam datasets, we used horizontal and vertical flip, random rotation, random crop and gamma.

Comparison of methods: We compared VAT with state-of-the-art Self-supervised methods such as SimCLR [30], Context Prediction (CP) [9], and Rotation [19]. We also provided an upper-boundary (UB) fully-supervised benchmark, which emulated the setup when all data is available for training. For all proposed methods, we reported the best performance obtained after optimizing the mixing coefficient λ .

Cross-validation strategy: For the ACDC dataset, we split the original data into X_{pre} (80 volumes) and X_{test} (20 volumes) subsets. For the limited annotation problem setups, we selected $X_{tr} = 2$, $X_{tr} = 4$, and $X_{tr} = 8$ 3D volumes from X_{pre} for model training, leaving 2 volumes for validation ($X_{val} = 2$). For the UB setup, we split X_{pre} into $X_{tr} = 60$ and $X_{val} = 20$ volumetric images. We applied the same splitting strategy for the APTOS experiment with $X_{test} = 733$, $X_{tr} = 59$, $X_{tr} = 122$, $X_{tr} = 234$, $X_{pre} = 2811$ and $X_{val} = 29$ images for the limited annotation problem setups, and $X_{tr} = 2343$, $X_{val} = 293$ and $X_{test} = 733$ for the UB setup. Finally, we split the PCam dataset into $X_{test} = 44005$, $X_{tr} = 22$, $X_{tr} = 44$, $X_{tr} = 83$, $X_{pre} = 175975$ and $X_{val} = 23$ images for the limited annotation experiments and $X_{tr} = 140816$, $X_{val} = 3521$ and $X_{test} = 44005$ for the UB experiments. For all experiments, we trained the model using X_{train} , using X_{val} for early stopping, and performed the final evaluation on the unseen X_{test} subsets.

Evaluation: Dice macro similarity (without background), Area Under the Receiver Operating Characteristic Curve (AUC-ROC), and quadratic weighted Kappa scores were used to evaluate the segmentation (ACDC), classification (PCam), and ordinary regression (APTOS) performance, respectively. For all experiments, we report the mean scores evaluated on the X_{test} subset over 5 runs.

4.2 Experimental results

A comparison of the proposed method (VAT) with state-of-the-art self-supervised methods is presented in Tables 2-4. VAT with late aggregation did not succeed in most experiments while the early aggregation technique provided strong results, outperforming the baseline models. As discussed above, we hypothesize that late aggregation does not provide explicit enough penalization of the feature representations, which leads to the de-synchronization of local and global feature representations during training and therefore, degradation of model performance.

Table 2: Comparison of the proposed method with pre-training methods, ACDC dataset.

Method	$X_{tr} = 2$	$X_{tr} = 4$	$X_{tr} = 8$	$X_{tr} = 60$ (UB)
Baseline	0.700	0.766	0.834	0.902
SimCLR	0.721	0.748	0.796	-
CP	0.743	0.790	0.799	-
Rotation	0.744	0.791	0.834	-
VAT, early agg. (ours)	0.749	0.814	0.834	-
VAT, late agg.(ours)	0.616	0.795	0.546	-

Table 3: Comparison of the proposed method with pre-training methods, APTOS dataset.

Method	$X_{tr} = 59$	$X_{tr} = 122$	$X_{tr} = 234$	$X_{tr} = 2343$ (UB)
Baseline	0.804	0.851	0.852	0.909
SimCLR	0.619	0.769	0.789	-
CP	0.822	0.847	0.849	-
Rotation	0.827	0.855	0.863	-
VAT, early agg. (ours)	0.851	0.863	0.868	-
VAT, late agg.(ours)	0.452	0.455	0.462	-

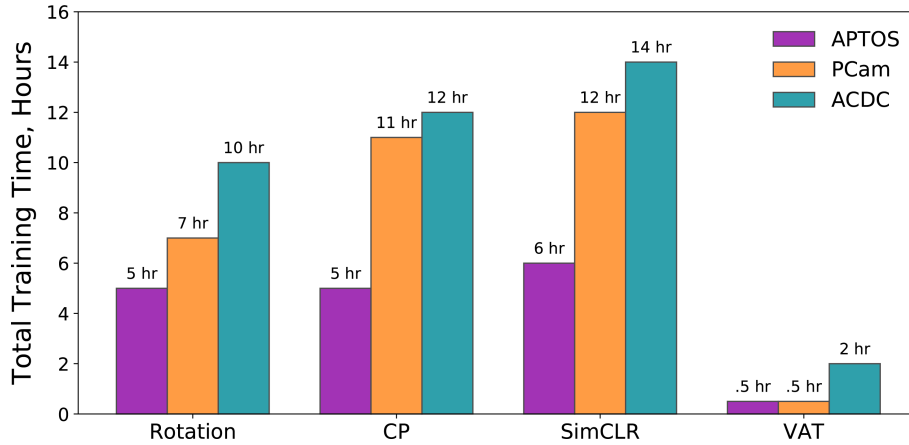
Table 4: Comparison of the proposed method with pre-training methods, PCam dataset.

Method	$X_{tr} = 22$	$X_{tr} = 44$	$X_{tr} = 83$	$X_{tr} = 140816$ (UB)
Baseline	0.776	0.745	0.726	0.989
SimCLR	0.781	0.817	0.860	-
CP	0.706	0.794	0.814	-
Rotation	0.739	0.760	0.824	-
VAT, early agg. (ours)	0.806	0.809	0.833	-
VAT, late agg.(ours)	0.796	0.777	0.822	-

Compared to the SSL methods, VAT either matched or surpassed the top SSL scores. SSL methods resulted in a range of performances on different tasks. SimCLR provided the best performance for the PCam experiment but failed on others resulting in a performance that was worse than the baseline model. Rotation and CP methods produced a strong performance on all tasks, improving the baseline, but VAT consistently matched or outperformed those methods. In total training GPU time, SSL pre-training and fine-tuning took more than 10 hours of GPU time on 2 RTX 2080 for all experiments, while VAT demonstrated almost the same training time as the baseline model, which was only 2 hours for ACDC and 0.5 hours for APTOS and PCam experiments (Figure 4).

Additionally, we faced the challenge of finding an optimal combination of hyper-parameters and augmentations for SSL pre-training tasks. In contrast, our method required only selecting the mixing coefficient λ and used the same augmentations and model architecture as the baseline solution. We suggest that combined with fast convergence, VAT could drastically decrease the time spent on model research.

We also empirically demonstrated that VAT does indeed minimize the model’s variance. The positive effect of introducing VAT into the baseline model decreases with the increase in the dataset size (Tables 2-3) and we found the same correlation with respect to the optimal mixing coefficient λ (Figures 4a-4f). In the general case for a model with a fixed capacity, the variance error decreases with an increase in the dataset size and therefore, it reduces the variance error of the model.

Figure 3: Comparison of the total training time of VAT method with self-supervised methods (pre-train and downstream tasks) for ACDC $X_{tr} = 8$, APTOS $X_{tr} = 234$, and PCam $X_{tr} = 83$ setups.

Furthermore, we found the PCam classification experiment extremely expressible of the VAT performance. When introducing more training examples, the AUC-ROC score degraded from 0.776 to 0.726 due to an increase in unrepresentable samples, which lead to over-fitting. In contrast, our method penalizes shifted feature representations, bringing back the positive correlation between the model’s performance and dataset size. Moreover, increasing the number of unrepresentable training samples increased the optimal λ (Figures 4g-4i), which supports our observations.

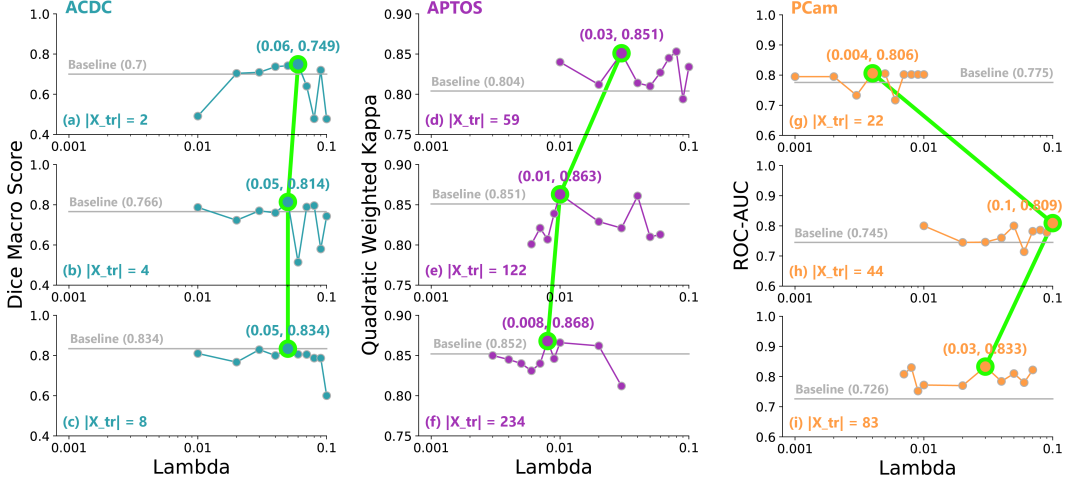


Figure 4: Exploration of the relationships between selected mixing coefficient λ and final model performance: (a), (b), (c) ACDC experiments; (d), (e), (f) APTOS experiments; (g), (h), (i) PCam experiments.

5 Limitations

The practical application of the proposed method is limited by the fundamental assumption of the morphological compactness of the training data. We assume that the approach will provide a poor performance when applied to computer vision problems with complex environmental setup (light, position of camera, diverse set of objects and camera pose) where bias error will be the dominant component of the BSTD. Additionally, since the proposed method requires storing twice as many gradients for the encoder, it increases GPU memory consumption compared to the baseline model, which could be a limitation for tasks requiring large models (for example, object detection) or large batch size.

6 Conclusion

In this paper, we proposed a novel method for medical imaging model training, called Variance-Aware Training, which focuses on the direct optimization of model estimation variance. Our contributions include both a theoretical formulation and an experimental analysis of the proposed method. As a result, we demonstrated that, compared to Self-Supervised methods, our approach achieved the same or superior performance without the need for pre-training, which resulted in a 4-11% improvement on various medical imaging tasks. In addition to these performance improvements, our method was able to significantly reduce the training time and simplify model development.

7 Acknowledgments

We would like to thank Animesh Garg for fruitful discussions and feedback on the draft. Also, we would like to thank Laussen Labs and SickKids Hospital for their support.

References

- [1] G. Cybenko. “Approximation by superpositions of a sigmoidal function”. In: *Mathematics of Control, Signals and Systems* 2 (1989), pp. 303–314.
- [2] J. Bromley et al. “Signature Verification Using A “Siamese” Time Delay Neural Network”. In: *Int. J. Pattern Recognit. Artif. Intell.* 1993.
- [3] Tom Heskes. “Bias/Variance Decompositions for Likelihood-Based Estimators”. In: *MIT Press* 10 (1998), pp. 1425–1433.
- [4] Li Fei-Fei, R. Fergus, and P. Perona. “A Bayesian approach to unsupervised one-shot learning of object categories”. In: *Proceedings Ninth IEEE International Conference on Computer Vision* (2003), 1134–1141 vol.2.
- [5] I. Goodfellow et al. “Generative Adversarial Nets”. In: *NIPS*. 2014.
- [6] Elad Hoffer and Nir Ailon. “Deep metric learning using Triplet network”. In: *arXiv preprint arXiv:1412.6622* (2014).
- [7] Nitish Srivastava et al. “Dropout: a simple way to prevent neural networks from overfitting”. In: *J. Mach. Learn. Res.* 15 (2014), pp. 1929–1958.
- [8] A. Blum, N. Haghtalab, and Ariel D. Procaccia. “Variational Dropout and the Local Reparameterization Trick”. In: *NIPS*. 2015.
- [9] Carl Doersch, A. Gupta, and Alexei A. Efros. “Unsupervised Visual Representation Learning by Context Prediction”. In: *2015 IEEE International Conference on Computer Vision (ICCV)* (2015), pp. 1422–1430.
- [10] Alexey Dosovitskiy et al. “Discriminative unsupervised feature learning with convolutional neural networks.” In: *In Advances in Neural Information Processing Systems 27 (NIPS), 2014*. 2015.
- [11] Diederik P. Kingma and Jimmy Ba. “Adam: A Method for Stochastic Optimization”. In: *CoRR* abs/1412.6980 (2015).
- [12] G. Koch, R. Zemel, and R. Salakhutdinov. “Siamese Neural Networks for One-shot Image Recognition”. In: *Proceedings of the 32 nd International Conference on Machine Learning, Lille, France, 2015. JMLR: W&CP volume 37*. 2015.
- [13] Mehdi Noroozi and Paolo Favaro. “Unsupervised Learning of Visual Representations by Solving Jigsaw Puzzles”. In: *arXiv preprint arXiv:1603.09246v2* (2016).
- [14] Wenjia Bai et al. “Semi-supervised Learning for Network-Based Cardiac MR Image Segmentation”. In: *MICCAI*. 2017.
- [15] Babak Ehteshami Bejnordi et al. “Diagnostic Assessment of Deep Learning Algorithms for Detection of Lymph Node Metastases in Women With Breast Cancer”. In: *JAMA* 318 (2017), pp. 2199–2210.
- [16] Amir Jamaludin, T. Kadir, and Andrew Zisserman. “Self-supervised Learning for Spinal MRIs”. In: *DLMIA/ML-CDS@MICCAI*. 2017.
- [17] Aiham Taleb, Christoph Lippert, and Tassilo Kleinand Moin Nabi. “Self-supervised Learning for Medical Image by Solving Multimodal Jigsaw Puzzles”. In: 2017. eprint: 1912.05396.
- [18] M. Zaheer et al. “Deep Sets”. In: *NIPS*. 2017.
- [19] Spyros Gidaris, Praveer Singh, and Nikos Komodakis. “Unsupervised Representation Learning by Predicting Image Rotations”. In: *ArXiv* abs/1803.07728 (2018).
- [20] Brady Neal et al. “A Modern Take on the Bias-Variance Tradeoff in Neural Networks”. In: *ArXiv* abs/1810.08591 (2018).
- [21] Yunhua Zhang et al. “Structured Siamese Network for Real-Time Visual Tracking”. In: *ECCV*. 2018.
- [22] Qiao Zheng et al. “3-D Consistent and Robust Segmentation of Cardiac Images by Deep Learning With Spatial Propagation”. In: *IEEE Transactions on Medical Imaging* 37 (2018), pp. 2137–2148.
- [23] XWenjia Bai et al. “Self-Supervised Learning for Cardiac MR Image Segmentation by Anatomical Position Prediction”. In: *Medical Image Computing and Computer Assisted Interventions (MICCAI)*. 2019.
- [24] Pak Lun Kevin Ding et al. “Deep residual dense U-Net for resolution enhancement in accelerated MRI acquisition”. In: *Medical Imaging: Image Processing*. 2019.

- [25] Byungju Kim et al. “Learning Not to Learn: Training Deep Neural Networks with Biased Data”. In: *Conference on Computer Vision and Pattern Recognition (CVPR)*. 2019.
- [26] B. Li et al. “SiamRPN++: Evolution of Siamese Visual Tracking With Very Deep Networks”. In: *2019 IEEE/CVF Conference on Computer Vision and Pattern Recognition (CVPR)* (2019), pp. 4277–4286.
- [27] Mingxing Tan and Quoc V. Le. “EfficientNet: Rethinking Model Scaling for Convolutional Neural Networks”. In: *ArXiv abs/1905.11946* (2019).
- [28] Qiang Wang et al. “Fast online object tracking and segmentation: A unifying approach”. In: *Proceedings of the IEEE conference on computer vision and pattern recognition*. 2019.
- [29] K. Chaitanya et al. “Contrastive learning of global and local features for medical image segmentation with limited annotations”. In: *ArXiv abs/2006.10511* (2020).
- [30] Ting Chen, Simon Kornblith, and Mohammad Norouzi, and Geoffrey Hinton. “A simple framework for contrastive learning of visual representations.” In: *arXiv*. 2020. eprint: 2002.05709.
- [31] Zhengyang Feng et al. “DMT: Dynamic Mutual Training for Semi-Supervised Learning”. In: 2020.
- [32] Benyamin Ghogh, Milad Sikaroudi, and Sobhan Shafiei. “Fisher Discriminant Triplet and Contrastive Losses for Training Siamese Networks”. In: *International Joint Conference on Neural Networks (IJCNN), IEEE, 2020*. 2020.
- [33] Y. Lu and J. Lu. “A Universal Approximation Theorem of Deep Neural Networks for Expressing Probability Distributions”. In: *arXiv: Learning* (2020).
- [34] Haggai Maron et al. “On Learning Sets of Symmetric Elements”. In: *ArXiv abs/2002.08599* (2020).
- [35] C. Ouyang et al. “Self-Supervision with Superpixels: Training Few-shot Medical Image Segmentation without Annotation”. In: *ECCV*. 2020.
- [36] B. Tymchenko, Philip Marchenko, and D. Spodarets. “Deep Learning Approach to Diabetic Retinopathy Detection”. In: *ArXiv abs/2003.02261* (2020).
- [37] D. Wang et al. “FocalMix: Semi-Supervised Learning for 3D Medical Image Detection”. In: *2020 IEEE/CVF Conference on Computer Vision and Pattern Recognition (CVPR)* (2020), pp. 3950–3959.
- [38] Zitong Yang et al. “Rethinking Bias-Variance Trade-off for Generalization of Neural Networks”. In: *ICML*. 2020.
- [39] Fatemeh Haghighi et al. *Transferable Visual Words: Exploiting the Semantics of Anatomical Patterns for Self-supervised Learning*. 2021. arXiv: 2102.10680 [cs.CV].
- [40] María Leyva-Vallina, Nicola Strisciuglio, and Nicolai Petkov. “Generalized Contrastive Optimization of Siamese Networks for Place Recognition”. In: *arXiv preprint arXiv:2103.06638* (2021).
- [41] Ru Li et al. “JigsawGAN: Self-supervised Learning for Solving Jigsaw Puzzles with Generative Adversarial Networks”. In: *arXiv preprint arXiv:2101.07555* (2021).
- [42] C. Srinidhi et al. “Self-supervised driven consistency training for annotation efficient histopathology image analysis”. In: *ArXiv abs/2102.03897* (2021).
- [43] *APTOS 2019 Blindness Detection*. URL: <https://www.kaggle.com/c/aptos2019-blindness-detection/overview/aptos-2019> (visited on 05/25/2020).
- [44] *Automated cardiac diagnosis challenge (acdc)*. URL: <https://www.creatis.insa-lyon.fr/Challenge/>.
- [45] Yaroslav Ganin et al. “Domain-Adversarial Training of Neural Networks.” In: *International Conference on Neural Information Processing Systems (NeurIPS)*. (2014).